Observation of Magnetic Ordering as High as 28 K for *meso*-Tetrakis(4-halophenyl)porphinatomanganese(III) Tetracyanoethenide, [MnTXPP][TCNE] (X = F, Br, I)

Durrell K. Rittenberg and Joel S. Miller*

Department of Chemistry, 315 South 1400 East RM Dock, University of Utah, Salt Lake City, Utah 84112-0850

Received February 10, 1999

The toluene solvates of *meso*-tetrakis(4-halophenyl)porphinatomanganese(III) tetracyanoethenide, [MnTFPP][TCNE] (**1F**), [MnTBrPP][TCNE] (**1Br**), and [MnTIPP][TCNE] (**1I**) have been prepared, and the magnetic and thermal properties have been determined and compared to those of [MnTClPP][TCNE] (**1Cl**). **1Br** and **1I** form uniform 1-D chains with each $[TCNE]^{\bullet-}$ being *trans*-μ-*N*-σ-bound to Mn^{III} with Mn−N distances of 2.293 (**1Br**) and 2.276 (**1I**), which are a bit longer than 2.267 Å observed for **1Cl**. The Mn−N−C angles are 167.2, 168.1, and 158.7, while intrachain Mn···Mn separations are 10.189, 10.277, and 10.101 Å. The magnetic susceptibilities for **1Br** and **1I** can be fit by the Curie−Weiss expression with high-temperature ($T > 200$ K) θ and low-temperature ($T < 110$ K) effective θ' values of −53 and 13 K and −79 and 30 K, respectively, compared to −60 and 13 K in **1Cl**. θ is not observed for **1F**; however, θ' is 70 K. The magnetic data are consistent with linear chain ferrimagnets composed of antiferromagnetically coupled $S = 2$ Mn^{III} sites and $S = {}^1/_2$ $[TCNE]^{\bullet-}$ sites with the antiferromagnetic intrachain coupling, J_{intra}/k_B (k_B = Boltzmann's constant) determined from fits to the Seiden expression, of −225, −33, −30, and −53 K for the **1F**, **1Cl**, **1Br**, and **1I**, respectively. Hysteresis with coercive fields at 2 K of 20.0, 6.7, 4.0, and 15.9 kOe was observed for the **1F**, **1Cl**, **1Br**, and **1I**, respectively. Metamagnetic behavior is observed below 10 K for **1F**, and below 5 K for both **1Br** and **1I**. The observed critical fields of 21.8, 6.8, 4.1, and 15.8 kOe were observed for **1F**, **1Cl**, **1Br**, and **1I** at 2 K, respectively. The ordering temperatures, T_c, determined from the maxima in the $\chi'(T)$ data taken at 10 Hz, are 28.0, 8.8, 8.0, and 6.5 K for **1F**, **1Cl**, **1Br**, and **1I**, respectively. The 28 K T_c for **1F** is the highest reported for this family of magnets.

Introduction

The establishment of structure−function relationships is critical to the advancement of the molecular sciences. Nowhere is this more apparent than in the area of materials science devoted to the preparation of molecule-based magnets.[1,2] The first organic-containing molecule-based magnet characterized was the electron-transfer salt $[FeCp_2^*]^{\bullet+}[TCNE]^{\bullet-}$ (Cp* = pentamethylcyclopentadienide; TCNE = tetracyanoethylene) with an ordering temperature, T_c, of 4.8 K.[3] Improvements led to the discovery of the first room temperature molecule-based magnet, the disordered $V(TCNE)_x{\cdot}y$solvent with a $T_c \sim 400$ K.[4] More recently, studies have focused on a class of metallomacrocycles and [TCNE]-based magnets exemplified by [MnTPP][TCNE]·2PhMe (TPP = *meso*-tetraphenylporphinato) with a T_c of 14 K.[5] Since then additional porphyrin-based magnets have been prepared and characterized; however, a complete understanding of the magnetic behavior of this class of materials is still under investigation.[6] Due to the relative ease of modifying

(1) Miller, J. S., Dougherty D. A., Eds. Proceedings on the Conference on Ferromagnetic and High Spin Molecular Based Materials. *Mol. Cryst. Liq. Cryst.* **1989**, *176*. Kahn, O., Gatteschi, D., Miller, J. S., Palacio, F., Eds. Proceedings on the Conference on Molecular Magnetic Materials. *NATO ARW Mol. Magn. Mater.*, **1991**, *E198*. Iwamura, H., Miller, J. S., Eds. Proceedings on the Conference on the Chemistry and Physics of Molecular Based Magnetic Materials. *Mol. Cryst. Liq. Cryst.* **1993**, *232/233*. Miller, J. S., Epstein, A. J., Eds. Proceedings on the Conference on Molecule-based Magnets. *Mol. Cryst. Liq. Cryst.* **1995**, *271−274*. Itoh, K., Miller, J. S., Takui, T., Eds. Proceedings on the Conference on Molecular-Based Magnets. *Mol. Cryst. Liq. Cryst.* **1997**, *305/306*. Turnbull, M. M., Sugimoto, T., Thompson, L. K., Eds. *ACS Symp. Ser.* **1996**, *644*.

(2) Reviews. (a) Buchachenko, A. L. *Russ. Chem. Rev.* **1990**, *59*, 307; *Usp. Khim.* **1990**, *59*, 529. Kahn, O. *Molecular Magnetism*; VCH Publishers: New York, 1993. (b) Caneschi, A.; Gatteschi, D.; Sessoli, R.; Rey, P. *Acc. Chem. Res.* **1989**, *22*, 392. D. Gatteschi, *Adv. Mater.* **1994**, *6*, 635. (c) Miller, J. S.; Epstein, A. J.; Reiff, W. M. *Acc. Chem. Res.* **1988**, *21*, 114. Miller, J. S.; Epstein, A. J.; Reiff, W. M. *Science* **1988**, *240*, 40. Miller, J. S.; Epstein, A. J.; Reiff, W. M. *Chem. Rev.* **1988**, *88*, 201. Miller, J. S.; Epstein, A. J. In *New Aspects of Organic Chemistry;* Yoshida, Z., Shiba, T., Ohshiro, Y., Eds.; VCH Publishers: New York, 1989; p 237. Miller, J. S.; Epstein, A. J. *Angew. Chem. Int. Ed. Engl.* **1994**, *33*, 385; *Angew. Chem.* **1994**, *106*, 399. Miller, J. S.; Epstein, A. J. *Adv. Chem. Ser.* **1995**, *245*, 161. Miller, J. S.; Epstein, A. J. *Chem. Eng. News* **1995**, *73* (No. 40), 30. Plass, W. *Chem. Unserer Zeit* **1998**, *32*, 323.

(3) Miller, J. S.; Calabrese, J. C.; Epstein, A. J.; Bigelow, R. W.; Zhang, J. H.; Reiff, W. M. *J. Chem. Soc., Chem. Commun.* **1986**, 1026. Miller, J. S.; Calabrese, J.; Rommelmann, H.; Chittipeddi, S.; Zhang, J.; Reiff, W.; Epstein, A. J. *J. Am. Chem. Soc.* **1987**, *109*, 769.

(4) Manriquez, J.; Yee, G.; Mclean, R. S.; Epstein, A. J.; Miller, J. S. *Science* **1991**, *252*, 1415. Epstein, A. J.; Miller, J. S. In *Proceedings of Nobel Symposium #NS-81, Conjugated Polymers and Related Materials: The Interconnection of Chemical and Electronic Structure*; Oxford University Press: Oxford, 1993; p 475. Salaneck, W. R., Lundström, I., Rånby, B., Eds. *Chim. Ind. (Milan)* **1993**, *75*, 185, 257. Miller, J. S.; Yee, G. T.; Manriquez, J. M.; Epstein, A. J. In *Proceedings of Nobel Symposium #NS-81, Conjugated Polymers and Related Materials: The Interconnection of Chemical and Electronic Structure*; Oxford University Press: Oxford, 1993; p 461. Salaneck, W. R., Lundström, I., Rånby, B., Eds. *Chim. Ind. (Milan)* **1992**, *74*, 845.

(5) (a) Miller, J. S.; Calabrese, J. C.; Mclean, R. S.; Epstein, A. J. *Adv. Mater.* **1992**, *4*, 498. (b) Zhou, P.; Morin, B. G.; Epstein, A. J.; McLean, R. S.; Miller, J. S. *J. Appl. Phys.* **1993**, *73*, 6569. (c) Brinckerhoff, W. B.; Morin, B. G.; Brandon, E. J. B.; Miller, J. S.; Epstein, A. J. *J. Appl. Phys.* **1996**, *79*, 6147.

(6) Miller, J. S.; Epstein, A. J. *Chem. Commun. (Cambridge)* **1998**, 1319.

10.1021/ic990170g CCC: $18.00
Published on Web 09/28/1999

the porphyrin structure, we[6−8] and others[9,10] have prepared a series of substituted tetraphenylporphyrin TCNE electron transfer salts with the hope of establishing a structure−function relationship.

Magneto−structural relationships have been established in bridged dinuclear metal complexes[11] and in extended liner chain compounds.[12] Until recently, establishing structure−function relationships for the [MnTPP][TCNE]·solvent system has proved difficult due to their structural complexity, the nature of which varies significantly depending on the substituents, and solvents used as well as structural disorder.[6] For example, five phases of [MnTClPP][TCNE] have been reported.[7e] A magneto−structural relationship correlating the intrachain (1-D) coupling, J_{intra}, with the Mn−N−C_{TCNE} angle and the dihedral angle between the MnN_4 and $[TCNE]^{\bullet-}$ mean planes was recently reported.[13] This correlation provides insight into the intrachain spin coupling mechanism; however, it fails to address the magnetic ordering as it neglects the necessary interchain (2- and 3-D) couplings, J_{inter}.

Simple two-spin systems can be described by the spin Hamiltonian, H:

$$H = -2J\mathbf{S}_1\cdot\mathbf{S}_2 \qquad (1)$$

where $\mathbf{S}_1$ and $\mathbf{S}_2$ are neighboring spin sites 1 and 2 and J is the exchange coupling between the two spins. The sign and magnitude of the exchange, J, depends largely upon the system studied. In [MnTPP][TCNE], J is dominated by the 1-D antiferromagnetic coupling between Mn^{III} and $[TCNE]^{\bullet-}$, which can be determined from modeling the data by the Seiden expression[14] for isolated chains of alternating classical $S = 2$ and quantum $S = {}^1/_2$ spins. Below 30 K, 2- and 3-D interactions begin to dominate and the Seiden model is no longer adequate. With no direct contact between chains, the dominant pathway of interchain exchange is primarily dipolar (through space) in nature; therefore, interchain coupling, J_{inter}, should exhibit significant distance dependence.[6,15] For an orthorhombic unit cell where the chains stack parallel to a principal axis, the ordering temperature, T_c, can be approximated by eq 2.[15]

$$T_c = S(S+1)[8|J_{intra}||J_{inter}|]^{1/2} \qquad (2)$$

To study the relatively weak interchain 2- and 3-D interactions, systems that exhibit similar intrachain couplings, in which the interchain couplings can be varied by small perturbations of r via changes in the interchain distances, were sought. The system targeted for study was *meso*-tetrakis(4-fluorophenyl)-porphinatomanganese(III) tetracyanoethenide, [Mn^{III}TFPP]-[TCNE]·PhMe (**1F**), *meso*-tetrakis(4-bromophenyl)porphinato-manganese(III) TCNE, [Mn^{III}TBrPP]-[TCNE]·2PhMe (**1Br**), and *meso*-tetrakis(4-iodophenylporphinato)manganese(III) TCNE, [Mn^{III}TIPP][TCNE]·2PhMe (**1I**), to complement the previous work on *meso*-tetrakis(4-chlorophenyl)porphinatomanganese-(III) TCNE,[7e] [Mn^{III}TClPP][TCNE]·2PhMe (**1Cl**), in order to establish a magneto−structural relationship. It was thought that this family might be isostructural and simplify the development of a magneto−structural relationship. Comparisons to previously reported **1H**[5] and *meso*-tetrakis(2-fluorophenyl)porphinatomanganese(III) tetracyanoethenide, [Mn^{III}ToFPP][TCNE]·2PhMe,[7f] were not made as these materials have sufficiently different solid state structures.

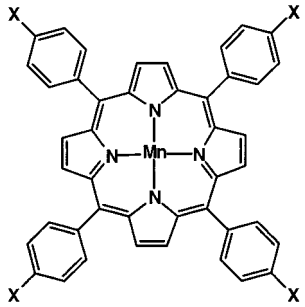

1F (X = F), **1Cl** (X = Cl), **1Br** (X = Br), **1Cl** (X = Cl), **1I** (X = I), **1H** (X = H)

Experimental Section

Synthesis. All manipulations involving $[TCNE]^{\bullet-}$ were carried out under nitrogen using standard Schlenk techniques or in a Vacuum Atmospheres DriLab. Solvents used for the preparation of the $[TCNE]^{\cdot-}$ salts were predried and distilled from appropriate drying agents. H_2-TXPP (X = F, Cl, Br, I) were prepared by the Alder−Longo method.[16] [Mn^{III}TXPP][OAc] complexes were prepared from H_2TXPP and Mn-$(OAc)_2\cdot 4H_2O$; the $Mn(OAc)_2\cdot 4H_2O$ was predissolved in *N*,*N*-dimethylformamide and filtered before addition to the free-base porphyrins, to remove paramagnetic impurities. The $[Mn^{III}TXPP]^+$ salts were subsequently reduced to Mn^{II}TXPP as the pyridine adducts, Mn^{II}TXPP-(py), by $NaBH_4$ utilizing a literature method.[17] TCNE was obtained as a gift from O. Webster and was resublimed prior to use. [Mn^{III}TClPP]-[TCNE]·2PhMe (**1Cl**) was prepared as previously reported.[7e]

[MnTFPP][TCNE]·*x*PhMe (**1F**) was prepared by the reaction of filtered solutions of Mn^{II}TFPP(py) (60.9 mg, 0.0741 mmol) dissolved

(7) (a) Böhm, A.; Vazquez, C.; McLean, R. S.; Calabrese, J. C.; Kalm, S. E.; Manson, J. L.; Epstein, A. J.; Miller, J. S.; *Inorg. Chem.* **1996**, *35*, 3083. (b) Sugiura, K.-i.; Arif, A.; Rittenberg, D. K.; Schweizer, J.; Öhrstrom, L. Epstein, A. J.; Miller, J. S. *Chem.−Eur. J.* **1997**, *3*, 138. (c) Brandon, E. J.; Sugiura, K.-i.; Arif, A. M.; Liable-Sands, A.; Rheingold, A. L.; Miller, J. S. *Mol. Cryst. Liq. Cryst.* **1997**, *305*, 269. (d) Brandon, E. J.; Burkhart, B. M.; Rogers, R. D.; Miller, J. S. *Chem.−Eur. J.* **1998**, *4*, 1938. (e) Brandon, E. J.; Rittenberg, D. K.; Arif, A. M.; Miller, J. S. *Inorg. Chem.* **1998**, *37*, 3376. (f) Brandon, E. J.; Arif, A. M.; Burkhart, B. M.; Miller, J. S. *Inorg. Chem.* **1998**, *37*, 2792. (g) Rittenberg, D. K.; Sugiura, K.-i.; Sakata, Y.; Guzei, I. A.; Rheingold, A. L.; Miller, J. S. *Chem.−Eur. J.* **1999**, *5*, 1874. (h) Brandon, E. J.; Arif, A. M.; Miller, J. S.; Sugiura, K.-i.; Burkhart, B. M. *Cryst. Eng.* **1998**, *1*, 97.
(8) Sugiura, K.-i.; Mikami, S.; Tanaka, T.; Sawada, M.; Manson, J. L.; Miller, J. S.; Sakata, Y. *Chem. Lett.* **1997**, 1071.
(9) (a) Griesar, K.; Anthanassopoulou, M. A.; Soto Bustamante, E. A.; Tomkowicz, Z.; Zaleski, A. J.; Haase, W. *Adv. Mater.* **1997**, *9*, 45. Griesar, K.; Anthanassopoulou, M. A.; Tomkowicz, Z.; Balanda, M. *Mol. Cryst. Liq Cryst.* **1997**, *306*, 57. (b) Winter, H.; Dormann, E.; Gompper, R.; Janner, R.; Kothrade, S.; Wagner, B.; Naarmann, H. *J. Magn. Magn. Mater.* **1995**, *140−144*, 1443. Winter, H.; Klemen, M.; Dormann, W.; Gompper, R.; Janner, R.; Kothrade, S.; Wagner, B. *Mol. Cryst. Liq. Cryst.* **1995**, *273*, 111. Klemen, M.; Wachter, C.; Winter, H.; Dormann, W.; Gompper, R.; Hermann, D. *Mol. Phys.* **1997**, *90*, 407.
(10) (a) Nagai, K.; Iyoda, T.; Fujishima, A.; Hashimoto, K. *Synth. Met.* **1997**, *85*, 1701. (b) Nagai, K.; Iyoda, T.; Fujishima, A.; Hashimoto, K. *Solid State Commun.* **1997**, *102*, 809. (c) Nagai, K.; Iyoda, T.; Fujishima, A.; Hashimoto, K. *Chem. Lett.* **1996**, 591.
(11) Crawford, V. H.; Richardson, H. W.; Wasson, J. R.; Hodgson, D. J.; Hatfield, W. E. *Inorg. Chem.* **1976**, *15*, 2107.
(12) Jongh, L. J. In *Magneto-Structural Correlations in Exchange Coupled Systems. Magneto-Structural Correlations in Extended Magnetic Chain Systems;* Willett, R. D., Gatteschi, D., Kahn, O., Eds.; NATO ASI Series; D. Reidel Publishing: New York, 1983; Vol. 140, p 1.
(13) (a) Brandon, E. J.; Kollmar, C.; Miller, J. S. *J. Am. Chem. Soc.* **1998**, *120*, 1822. (b) Miller, J. S.; Brandon, E. J. In *NATO ARW Supramolecular Engineering of Synthetic Metallic Materials: Conductors and Magnets;* Veciana, J., Rovira, C., Amabilino, D., Eds.; Kluwer Acad. Pub.: Dordrecht, The Netherlands, 1998; Vol. C518, p 197.
(14) Seiden, J. *Phys. Lett.* **1983**, *44*, L947.
(15) Wynn, C. M.; Gîrtu, M. A.; Brinckerhoff, W. B.; Sugiura, K.-i.; Miller, J. S.; Epstein, A. J. *Chem. Mater.* **1997**, *9*, 2156.
(16) Alder, A. D.; Longo, F. R.; Finarelli, J. D.; Goldmacher, J.; Korsakoff, L. *J. Org. Chem.* **1967**, *32*, 476.
(17) Jones, R. D.; Summerville, D. A.; Basolo, F. *J. Am. Chem. Soc.* **1978**, *100*, 446.

in 50 mL of toluene and TCNE (15.9 mg, 0.12 mmol) dissolved in 10 mL of dichloromethane. The two solutions were mixed and allowed to stand at room temperature for 4 days in an inert atmosphere glovebox. The resulting dark-green precipitate was filtered off, washed three times with 10 mL portions of fresh, dry toluene, and dried in vacuo for 1.5 h at room temperature [yield: 51.1 mg (79%)]. Attempts to prepare crystals suitable for X-ray analysis were unsuccessful. IR (Nujol; cm^{-1}): ν_{CN} 2195 (m), 2135 (s). Anal. Calcd for [MnTFPP][TCNE] ($C_{50}H_{24}F_4MnN_8$), molecular weight 867.71 g/mol: C, 69.21; H, 2.79; N, 12.91. Found: C, 68.89; H, 3.01; N, 12.82. TGA/MS for a nondesolvated sample: 11.16% at 197 °C (z^+/e = 91 amu, toluene) corresponding to 1.18 PhMe.

[MnTBrPP][TCNE]·2PhMe (**1Br**) was prepared by the reaction of filtered solutions of Mn^{II}TBrPP(py) (23.3 mg, 0.0219 mmol) dissolved in 10 mL of toluene and TCNE (14.2 mg, 0.11 mmol) dissolved in 10 mL of dichloromethane. The two solutions were mixed and allowed to stand at room temperature for 4 days in an inert atmosphere glovebox. The resulting dark-green plate crystals were filtered off, washed three times with 10 mL portions of fresh, dry toluene, and dried in vacuo for 1.5 h at room temperature [yield: 27.3 mg (96%)]. Crystals suitable for X-ray diffraction were obtained by slow diffusion in an H-tube crystallization cell, which gave large plates (0.25 × 0.25 × 0.20 mm). IR (Nujol; cm^{-1}): ν_{CN} 2201 (m), 2160 (s), 2125 (vw). Anal. Calcd for [MnTBrPP][TCNE]·2PhMe ($C_{60}H_{40}Br_4MnN_8$) molecular weight 1295.61 g/mol: C, 59.33; H, 3.11; N, 8.65. Found: C, 59.53; H, 3.28; N, 8.44. TGA/MS 14.17% at 98 °C (z^+/e = 91 amu, toluene) corresponding to 1.99 PhMe.

[MnTIPP][TCNE]·2PhMe (1I). MnTIPP(py) (38.8 mg, 0.0310 mmol) was dissolved with stirring at room temperature in 15 mL of toluene, and the dark green solution was filtered through a medium glass-frit funnel. Excess TCNE (15.9 mg, 0.133 mmol) was dissolved in 20 mL of toluene, and the clear yellow solution was similarly filtered. The above two solutions were mixed and allowed to stand for 4 days in an inert atmosphere glovebox. The resulting precipitate was collected on a filter and washed three times with 10 mL portions of fresh toluene. The solid was dried in vacuo for 1.5 h, yielding 41.5 mg (92%) of dark-green microcrystals. Single crystals of **1I** were obtained by slow diffusion in an H-tube loaded with MnTIPP(py) dissolved in CH_2Cl_2 and layered with toluene. The crystals formed as very thin plates (0.25 × 0.17 × 0.005 mm) which diffracted very strongly. Anal. Calcd for [MnTIPP][TCNE]·2PhMe ($C_{64}H_{40}I_4MnN_8$), molecular weight, 1483.61 g/mol: C, 51.81; H, 2.72; N, 7.55. Found: C, 52.27; H, 2.94; N, 7.12. IR (Nujol; cm^{-1}): ν_{CN} 2203 (m), 2164 (s), 2125 (vw). TGA/MS 13.90% at 115 °C (z^+/e = 91 amu, toluene) corresponding to 2.28 PhMe.

Physical Methods. The 2−300 K dc magnetic susceptibility was determined on the equivalent of a Quantum Design MPMS-5XL 5 T SQUID (sensitivity = 10^{-8} emu or 10^{-12} emu/Oe at 1 T) magnetometer with an ultralow field (1 mOe) option, an ac option enabling the study of the ac magnetic susceptibility (χ' and χ'') in the range 10−1000 Hz, a reciprocating sample measurement system, and continuous low-temperature control with enhanced thermometry features. Samples were loaded in gelatin capsules or in an airtight Delrin holder and packed with oven-dried quartz wool and excess toluene (to prevent movement of the sample in the holder). For isofield dc measurements, the samples were zero-field cooled (following oscillation of the dc field), and data were collected upon warming. For ac measurements, remnant fluxes were minimized by oscillation of the dc field, with the sample cooled in zero applied field with data then taken upon warming. In addition to correcting for the diamagnetic contribution from the sample holder, core diamagnetic corrections of −454.7, −478.7, −540.7, −604.7 −60.0, −52.0, and −47 × 10^{-6} emu/mol were used for MnTFPP, MnTClPP, MnTBrPP, MnTIPP, TCNE, PhMe, and CH_2Cl_2, respectively. Infrared spectra (600−4000 cm^{-1}) were obtained on a Bio-Rad FT-40 spectrophotometer in mineral oil mulls. The thermal properties were studied on a TA Instruments model 2050 thermogravimetric analyzer (TGA) equipped with a TA-MS Fison triple-filter quadrupole mass spectrometer, to identify gaseous products with masses less than 300 amu, located in a Vacuum Atmospheres DriLab under argon to protect air- and moisture-sensitive samples. Samples were placed in an aluminum pan and heated at 20 °C/min under a continuous 10 mL/min nitrogen flow. Elemental analyses were performed by Atlantic Microlabs, Norcross, GA.

Table 1. Crystallographic Data for [MnTXPP][TCNE]·2PhMe (X = Cl (1Cl), Br (1Br), I(1I)]

	1Cl[a]	**1Br**	**1I**
formula	$C_{64}H_{40}Cl_4MnN_8$	$C_{64}H_{40}Br_4MnN_8$	$C_{64}H_{40}I_4MnN_8$
fw	1117.78	1295.62	1483.61
space group	$P\bar{1}$	$P\bar{1}$	$P\bar{1}$
a, Å	10.171(4)	10.0790(3)	9.8305(2)
b, Å	10.189(3)	10.2770(2)	10.1012(3)
c, Å	14.522(3)	14.6260(4)	15.3990(6)
α, deg	107.51(2)	73.1830(15)	81.0748(17)
β, deg	85.58(2)	84.3080(11)	79.6338(18)
γ, deg	111.51(3)	68.9920(15)	72.7559(18)
Z	1	1	1
V, Å^3	1334.4(7)	1353.79(6)	1428.90(8)
μ (empirical), mm^{-1}	4.98	3.246	2.441
ρ_{calcd}, g cm^{-3}	1.391	1.589	1.725
$R(F_o)$[b]	0.0426	0.043	0.0391
$R_w(F_o)$[c]	0.0831	0.1192	0.0929
temp, K	193	200	200
λ, Å	0.710 730	0.710 730	0.710 730

[a] Reference 7e. [b] $\sum w(|F_o| - |F_c|)/\sum|F_o^2|$. [c] $\{\sum w[F_o^2 - F_c^2]^2/\sum w[F_o^2]^2\}^{1/2}$.

X-ray Structure Determination. Cell constants and an orientation matrix for data collection for **1Br**·2PhMe and **1I**·2PhMe were obtained from 10 images exposed for 30 s at 200 K on a Nonius Kappa CCD diffractometer. The systematic absences uniquely determine the space group $P\bar{1}$ for both crystals. The structures were solved by direct methods and expanded using Fourier techniques using the SIR92[18] software package. The non-hydrogen atoms were refined anisotropically, and hydrogen atoms were included, but not refined, using SHELX97-2[19] as part of the WinGX[20] graphics suite. The final cycle of full-matrix least-squares refinement for **1Br**·2PhMe was based on 4563 observed reflections [$I_o > 2.00\sigma(I)$] and 366 variable parameters and converged with unweighted and weighted agreement factors R1 = 0.0434 and wR2 = 0.1192, respectively. The final cycle of full-matrix least-squares refinement for **1I**·2PhMe was based on 4832 observed reflections [$I_o > 2.00\sigma(I)$] and 337 variable parameters and converged with unweighted and weighted agreement factors R1 = 0.0391 and wR2 = 0.0929, respectively. Crystallographic details for **1Br**·2PhMe and **1I**·2PhMe are summarized in Table 1, and tables of the atomic coordinates, anisotropic thermal parameters, and bond angles are provided as Supporting Information.

Results and Discussion

The synthesis of [Mn^{III}TXPP][TCNE]·xPhMe (X = F, Cl, Br, I) was achieved from the reaction of Mn^{II}TXPPpy and TCNE in a mixture of dichloromethane and toluene. [MnTFPP][TCNE]·*x*PhMe, **1F**, [MnTClPP][TCNE]·2PhMe,[7e] **1Cl**, [MnTBrPP][TCNE]·2PhMe, **1Br**, and [MnTIPP][TCNE]·2PhMe, **1I**, were obtained as dark green platelike microcrystals with characteristic $[TCNE]^{\bullet-}$ ν_{CN} stretching frequencies, summarized in Table 2. In each case, the ν_{CN} absorptions are consistent with the presence of $[TCNE]^{\bullet-}$ as indicated by the large shifts to lower energy from 2259 (m) and 2221 (s) cm^{-1} for neutral TCNE and are comparable to that reported for [Bu_4N][TCNE].[21] **1Cl**, **1Br**, and **1I** exhibit bands at 2201 ± 2 (m), 2160 ± 3 (s), and 2125 ± 1 (vw) cm^{-1}, suggesting that they bond similarly to Mn^{III}. In contrast, 1F has ν_{CN} absorptions at 2195 (s) and 2137 (m) cm^{-1}.

(18) Altomare, A.; Cascarano, G.; Giacovazzo, C.; Guagliardi, A. SIR92—A program for crystal structure solution. *J. Appl. Crystallogr.* **1993**, *26*, 343.
(19) Sheldrick, G. M. *SHELX97-2 Programs for Crystal Structure Analysis (Release 97-2)*; University of Göttingen: Göttingen, Germany, **1998**.
(20) Farrugia, L. J. *WinGX—A Windows Program for Crystal Structure Analysis*. University of Glasgow: Glasgow, 1998.
(21) Dixon, D. A.; Miller, J. S. *J. Am. Chem. Soc.* **1987**, *109*, 3656. Stanley, J.; Smith, D.; Lattimer, B.; Delvin, J. P. *J. Phys. Chem.* **1966**, *70*, 2201.

Table 2. Infrared TCNE Stretching Data for [MnTXPP][TCNE]·*x*PhMe (X = F, Cl, Br, I)

compd	high ν_{CN}, cm^{-1} (m)	low ν_{CN}, cm^{-1} (s)	ν_{CN} shoulder, cm^{-1} (vw)
[MnTFPP][TCNE]	2195	2135	
[MnTClPP][TCNE][a]	2203	2163	2124
[MnTBrPP][TCNE]	2201	2160	2125
[MnTIPP][TCNE]	2204	2163	2125
[MnTPP][TCNE][b]	2192	2147	
$TCNE^0$ [c]	2259	2221	

[a] Reference 7. [b] Reference 5a. [c] Reference 22a.

The high-energy ν_{CN} absorption is believed to be the unbound nitrile and as such is invariant to coordination environment about Mn. As noted for **1Cl**, **1Br**, and **1I**, the low-energy nitrile absorption exhibits a wider range of energies varying by as much as 30 cm^{-1}. Hence, **1F** is structurally different from **1Cl**, **1Br**, and **1I**.

The nature and amount of the solvent present in [Mn^{III}TXPP][TCNE]·*x*PhMe were determined by thermogravimetric analysis coupled with electron spray mass spectra, TGA/MS. Initial weight losses were observed near room temperature for **1Cl**, **1Br**, and **1I** continuing to about 275 °C, with **1F** exhibiting initial weight loss near 200 °C. In all cases the weight losses were accompanied the appearance of toluene in the mass spectra. The observed toluene losses and predicted solvent content for **1F**, **1Cl**, **1Br**, and **1I** are 1.18, 1.78, 1.99, and 2.28 equiv, respectively. The temperature at which solvent loss occurs for **1F** is significantly higher than that for **1Cl**, **1Br**, and **1I**, suggesting that the solvent is held in the lattice more tightly, probably due to possible hydrogen bonding with fluorine or to solvent molecules' being "caged in" to a greater extent. Interestingly, **1F** intercalates less toluene (~1.2/Mn) compared with **1Cl**, **1Br**, and **1I** [(~2.0 ± 0.2)/Mn] possibly due to contraction of the lattice or close interchain spacing for the former.

Structure. The structures of **1Br** and **1I** were determined and are similar, but not isomorphous, to [MnTClPP][TCNE]·2PhMe, with Mn occupying a special position sitting on a center of inversion with the $[TCNE]^{\bullet-}$ also on an inversion center, Figure 1, Table 1. Disorder in the orientation of the toluene solvent was observed in both compounds. In **1Br**, Mn is in an axially distorted octahedral coordination environment with the $[TCNE]^{\bullet-}$ N sitting directly above the Mn−porphyrin plane with N(3)−Mn−N(1) and N(4)−Mn−N(1) bond angles of 89.99(12)° and 89.23(12)°, respectively. Similar coordination geometry was observed in **1I** with one notable difference: the $[TCNE]^{\bullet-}$ N is not directly centered above the porphyrin plane; rather the N(3)−Mn−N(1) and N(4)−Mn−N(1) bond angles are 92.55(15)° and 87.45(15)°, respectively. Mn−N_{TCNE} bond distances for **1Br** and **1I** are 2.293(3) and 2.276(4) Å, respectively, close to the distance of 2.267(3) Å found for **1Cl** and shorter than that of 2.305 Å for [MnTPP][TCNE]·2PhMe.[5a] The Mn−N_{ring} bond distances are 2.009(3) and 2.011(3) Å (**1Br**) and 2.010(3) and 2.013(4) Å (**1I**) and average 2.011 Å, with the remaining bond distances and angles typical of other [Mn^{III}TPP]$^+$ salts.[5a,7,22] As with the majority of $[TCNE]^{\bullet-}$ coordination polymer structures, $[TCNE]^{\bullet-}$ is planar with a twist of 0.0° for **1Cl**,[7e] **1Br**, and **1I**. The $[TCNE]^{\bullet-}$ bond distances for **1Br** and **1I** are summarized in Table 3 and are consistent with other known $[TCNE]^{\bullet-}$ structures.[5−7,23]

The solid state motifs of **1Br** and **1I**, like **1Cl**, are composed of similar 1-D chains of ···$D^+A^-D^+A^-$··· (D = MnTXPP; A = TCNE) where the TCNE is *trans*-*μ*-*N*-*σ*-bound to Mn which stack along *b*, Figures 2−4. The 168.1(3)° Mn−N−C bond angle for **1Br** is close to that reported for **1Cl** [167.2(3)°],[7e] but is significantly larger than that for **1I** [158.7(4)°]. Likewise, the dihedralangles between the mean planes of $[MnTXPP]^+$ and $[TCNE]^{\bullet-}$ are 86.8,[7e] 89.4°, and 69.6° for **1Cl**, **1Br**, and **1I**, respectively. The similar intrachain Mn···Mn separations of 10.189, 10.277, and 10.101 Å for **1Cl**, **1Br**, and **1I**, respectively, are close to that for [MnTPP][TCNE] (10.116 Å) and substantially larger than that for [MnTP′P][TCNE][7a] [H_2TP′P = tetrakis(3,5-di-*tert*-butyl-4-hydroxyphenyl)porphyrin] (8.587 Å). Unfortunately, attempts to grow crystals of **1F** suitable for single-crystal X-ray studies have not been successful.

Along *a*, the chains interdigitate with the phenyl groups on each adjacent chain pointing between the porphyrin planes of the closest chain to form 2-D sheets parallel to the *a* axis, Figure **2**. Close contacts were observed between the halogen X(1) and C(1) of $[TCNE]^{\bullet-}$ of 3.371, 3.481, and 3.848 Å for **1Cl**,[7e] **1Br**, and **1I**, respectively, Figures 3 and 4. The resulting 2-D sheets stack along *c* separated by columns of solvent, Figure 2. Important interchain and interlayer Mn···Mn interactions are listed in Table 4 and depicted in Figures 3 and 4. At low temperatures strong antiferromagnetic coupling between $[TCNE]^{\bullet-}$ and Mn^{III} dominate; thus the resulting spin is likely localized on Mn. NMR analysis has shown the spin density of Mn^{III}TPP(Cl) to be localized on the Mn center (2.87 μ_B) with less than 0.09 μ_B on the pyrrole nitrogen and 0.03 μ_B on the pyrrole carbon.[24] With the significant majority of the spin density (72%) localized on each Mn center, we assume that the interchain Mn···Mn distances are primarily responsible for 2- and 3-D magnetic ordering.

Magnetic Properties. The 2−300 K reciprocal corrected magnetic susceptibility (χ^{-1}) and effective moment, μ_{eff} [$\equiv(8\chi T)^{1/2}$], of **1F**, **1Cl**,[7e] **1Br**, and **1I** are presented in Figure 5 and are summarized in Table 5. The room temperature effective moments range from 4.69 to 5.44 μ_B which are close to the calculated spin-only value of 5.20 μ_B, for a system composed of noninteracting $g = 2$ $S = 2$ and $S = {}^1/_2$ spin sites and are typical for this class of materials.[5−7] Values below 5.20 μ_B result from antiferromagnetic coupling still present at room temperature, while the genesis of the 5.44 μ_B value is unknown, but may arise from uncertainty in the molecular weight (related to the specific degree of solvation).

The susceptibilities for all compounds can be fit by the Curie−Weiss expression, $\chi \propto 1/(T - \theta)$. As noted for **1Cl**,[7e] the data for **1Br** and **1I** have two linear regions that can be fit to this expression. For **1Br**, θ is −53 K for data above 250 K, while θ' is 13 K for data taken between 40 and 100 K, whereas for **1I**, θ is −79 K for data above 180 K, while θ' is 30 K for data taken between 70 and 130 K. The latter, ferromagnetic 13

(22) Day, V. W.; Sults, B. R.; Tasset, E. L.; Marianelli, R. S.; Boucher, L. J. *Inorg. Nucl. Chem. Lett.* **1975**, *11*, 505. Cheng, B.; Cukiernik, F.; Fries, P.; Marchon, J.-C.; Scheidt, W. R. *Inorg. Chem.* **1995**, *34*, 4627. (d) Guildard, R.; Perie, K.; Barbe, J.-M.; Nurco, D. J.; Smith, K. M.; Caemelbecke, E. V.; Kadish, K. M. *Inorg. Chem.* **1998**, *37*, 973. Landrum, J. T.; Hatano, K.; Scheidt, W. R.; Reed, C. A. *J. Am. Chem. Soc.* **1980**, *102*, 6729. Hill, C. L.; Williamson, M. M. *Inorg. Chem.* **1985**, *24*, 2834, 3024. Fleischer, E. B. *Acc. Chem. Res.* **1970**, *3*, 105. Scheidt, W. R.; Reed, C. A. *Chem. Rev.* **1981**, *81*, 543. Turner, P.; Gunter, M. J.; Hambley, T. W.; White, A. H.; Skelton, B. W. *Inorg. Chem.* **1992**, *31*, 2297.

(23) (a) Becker, P.; Coppens, P.; Ross, R. K. *J. Am. Chem. Soc.* **1973**, *95*, 7604. (b) Zheludev, A.; Grand, A.; Ressouche, E.; Schweizer, J.; Morin, B. G.; Epstein, A. J.; Dixon, D. A.; Miller, J. S. *J. Am. Chem. Soc.* **1994**, *116*, 7243.

(24) Mun, S. K.; Mallick, M. K.; Mishra, S.; Chang, J. C.; Das, T. P. *J. Am. Chem. Soc.* **1981**, *103*, 5024.

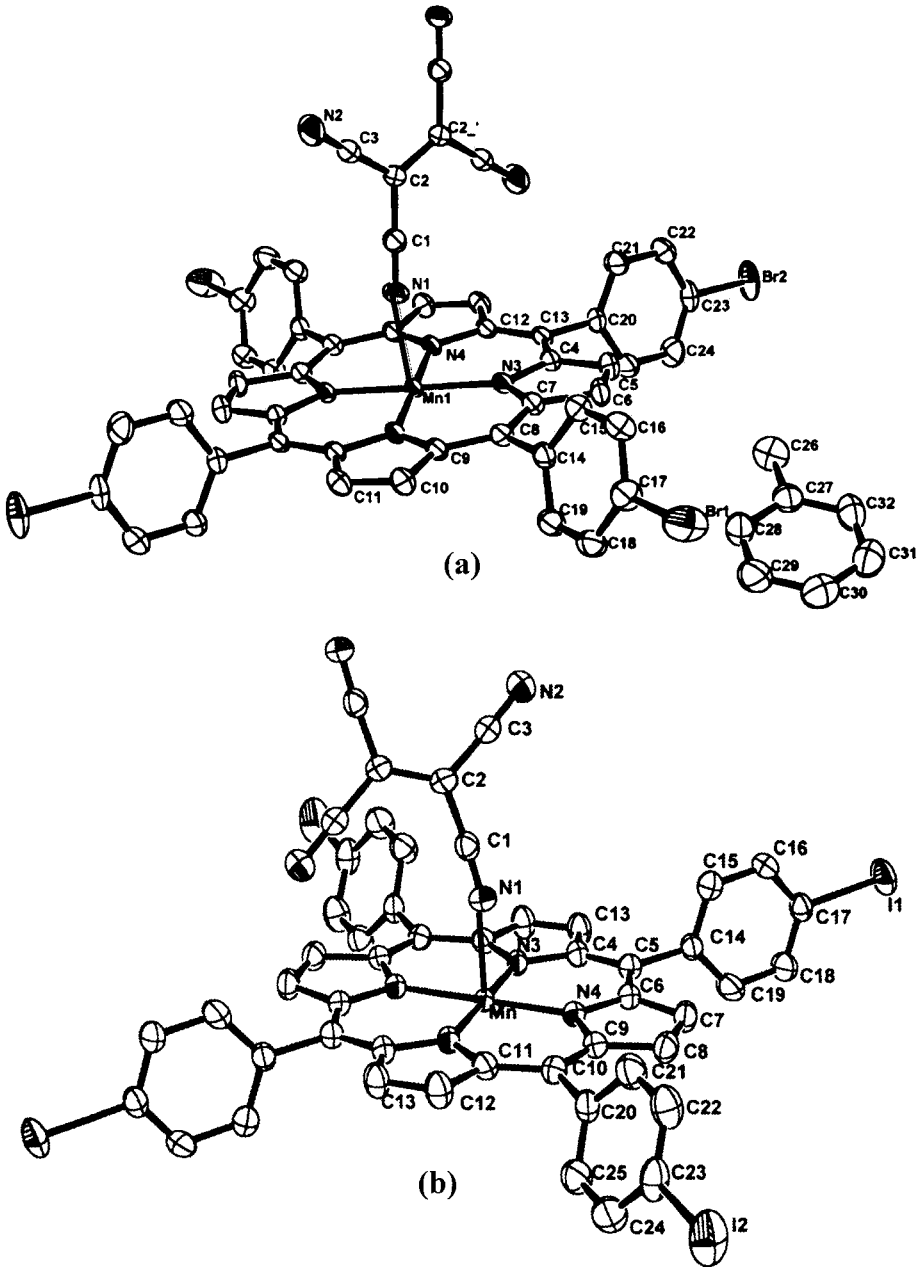

Figure 1. Labeling diagram and ORTEP (50% probability level) diagram for [MnTBrPP][TCNE]·2PhMe (**1Br**) (a) and [MnTClPP][TCNE]·2PhMe (**1I**) (b).

Table 3. $[TCNE]^{\bullet-}$ Bond Distances (Å) for Representative Compounds

	MnN−C	N−C	MnNC−C	NC−C	C−C
[MnTPP][TCNE][a]	1.153(4)	1.169(5)	1.392(5)	1.396(5)	1.426(7)
[MnTClPP][TCNE][b]	1.144(4)	1.142(4)	1.404(4)	1.418(8)	1.406(6)
[MnTBrPP][TCNE]	1.145(5)	1.143(5)	1.409(5)	1.416(5)	1.423(7)
[MnTIPP][TCNE]	1.134(6)	1.146(7)	1.416(7)	1.414(9)	1.405(9)
$TCNE^{0}$ [c]		1.117(5)		1.439(2)	1.344(4)
$[TCNE]^{\bullet-}$ [d]		1.170		1.406	1.429(8)

[a] Reference 5a. [b] Reference 7e. [c] Reference 22a. [d] Reference 22b.

and 30 K values are not the intrinsic θ values, but reflect a second, lower temperature linear region for $\chi^{-1}(T)$ and hence are termed effective θ, θ'.[7e] **1F** does not have a determinable θ value as data must be acquired at higher temperature. A θ' value of 70 K for **1F** is observed and reflects stronger magnetic couplings with respect to **1Cl**, **1Br**, and **1I**. The initial negative θ values along with the observation of broad minimums in the $\chi T(T)$ for **1Cl**, **1Br**, and **1I**, respectively, are consistent with the ferrimagnetic linear chains reported for α-[MnTClPP][TCNE],[7e] β-[MnTClPP][TCNE],[7e] *meso*-tetrakis(4-methoxyphenyl)porphinatomanganese(III) tetracyanoethenide, [MnTOMePP][TCNE],[7f] and [MnToFPP][TCNE].[7f] The absence of an observed minimum in $\chi T(T)$, or initial negative θ value in **1F** reflects stronger intrachain coupling with respect to **1Cl**, **1Br**, and **1I**, but it is consistent with [MnTPP][TCNE],[5] [MnTP′P][TCNE],[7a] and γ-[MnTClPP][TCNE][7e] which do not have a determinable θ for data taken up to 400 K.

Previously, an inverse correlation between θ' and both the dihedral angle between the mean MnN_4 and $[TCNE]^{\bullet-}$ mean planes and the Mn−N−C angle was established.[13] Hence, the relatively high 70 K θ' value suggests reduced angles with respect to **1Cl**, **1Br**, and **1I**. On the basis of this correlation **1F** is predicted to have an ∼36° dihedral angle and ∼150° Mn−N−C angle. Confirmation, however, must await its structure determination. The data for **1Cl** and **1Br** are in accord with this correlation; however, the expected values of 75° and 163°

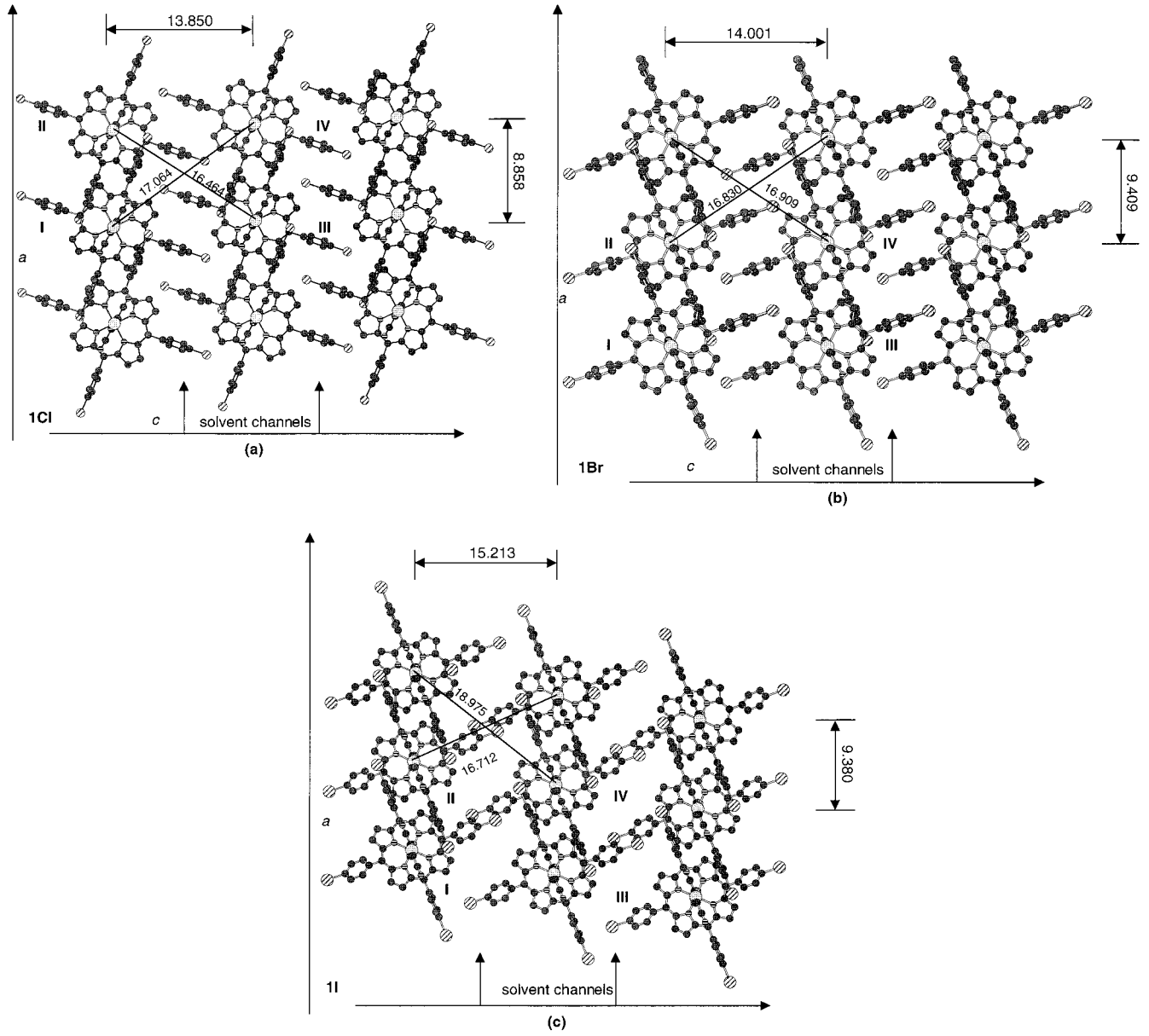

Figure 2. View down the *b* (chain) axis showing the proposed sheet structure of [MnTClPP][TCNE]·2PhMe (**1Cl**) (a), [MnTBrPP][TCNE]·2PhMe (**1Br**) (b), and [MnTIPP][TCNE]·2PhMe (**1I**) (c). Sheets are separated by columns of toluene, which have been omitted for clarity.

for the dihedral and Mn−N−C angles are in poor agreement with the observed values of 69.6° and 158.7°, respectively. This discrepancy is attributed to a structural difference, namely, for **1I** the $[TCNE]^{\bullet-}$ N is not directly centered above the porphyrin plane as observed for **1Cl** and **1Br**.

The ferrimagnetic nature of this class of magnets is evident from the minimum, T_{min}, albeit shallow, in $\mu(T)$ and $\chi T(T)$,[25] Figures 5 and 6, which occur at 80 K (**1Br**) to above room temperature for **1F**, Table 5. Due to the shallowness of the minimum as well as slight variations that occur between samples, the accuracy of T_{min} is estimated at ±20 K. Like θ', T_{min} correlates monotonically with magnetic coupling, Table 5.[13] T_{min} is model independent, but cannot be observed for strongly coupled systems as it occurs at temperatures exceeding the experimental range.

The $\chi T(T)$ data was modeled using a least-squares fit to an analytical expression for isolated chains composed of alternating classical $S = 2$ (Mn^{III}TXPP) and quantum $S = {}^1/_2$ ($[TCNE]^{\bullet-}$) spin sites derived by Seiden[14] to solely estimate the intrachain coupling, J_{intra}, Figure 6. At low temperatures the data deviates from the model due to the onset of 2- or 3-D interchain interactions which may be either ferromagnetic or antiferromagnetic. All compounds studied herein deviate from the Seiden prediction at lower temperatures consistent with ferromagnetic coupling as also noted for **1H**[5] and [MnTP′P][TCNE]·2PhMe,[7a] but not [MnOEP][$C_4(CN)_6$].[26] However, due to poor fitting of the data, quantitative fits to the Seiden function for **1H**[5] and [MnTP′P][TCNE]·2PhMe[7a] have not been made.

The best fit to the Seiden model[14] (using $H = -2J_{intra}\mathbf{S}_a\cdot\mathbf{S}_b$ and $g = 2$) yielded J_{intra} of −225, −33,[7e] −30, and −53 K for

(25) Coronado, E.; Drillon, M.; Georges, R. In *Research Frontiers in Magnetochemistry*; O'Connor, C. J., Ed.; World Scientific: Singapore, 1993; p 26. Beltran, D.; Drillon, M.; Coronado, E.; Georges, R. *Stud. Inorg. Chem.* **1983**, *3*, 589. Drillon, M.; Coronado, E.; Beltran, D.; Georges, R. *Chem. Phys.* **1983**, *79*, 449. Verdaguer, M.; Julve, M.; Michalowicz, A.; Kahn, O. *Inorg. Chem.* **1983**, *22*, 2624. Drillon, M.; Gianduzzo, J. C.; Georges, R. *Phys. Lett. A* **1983**, *96A*, 413.

(26) Miller, J. S.; C. Vazquez, C.; Jones, N. L.; McLean, R. S.; Epstein, A. J. *J. Mater. Chem.* **1995**, *5*, 707.

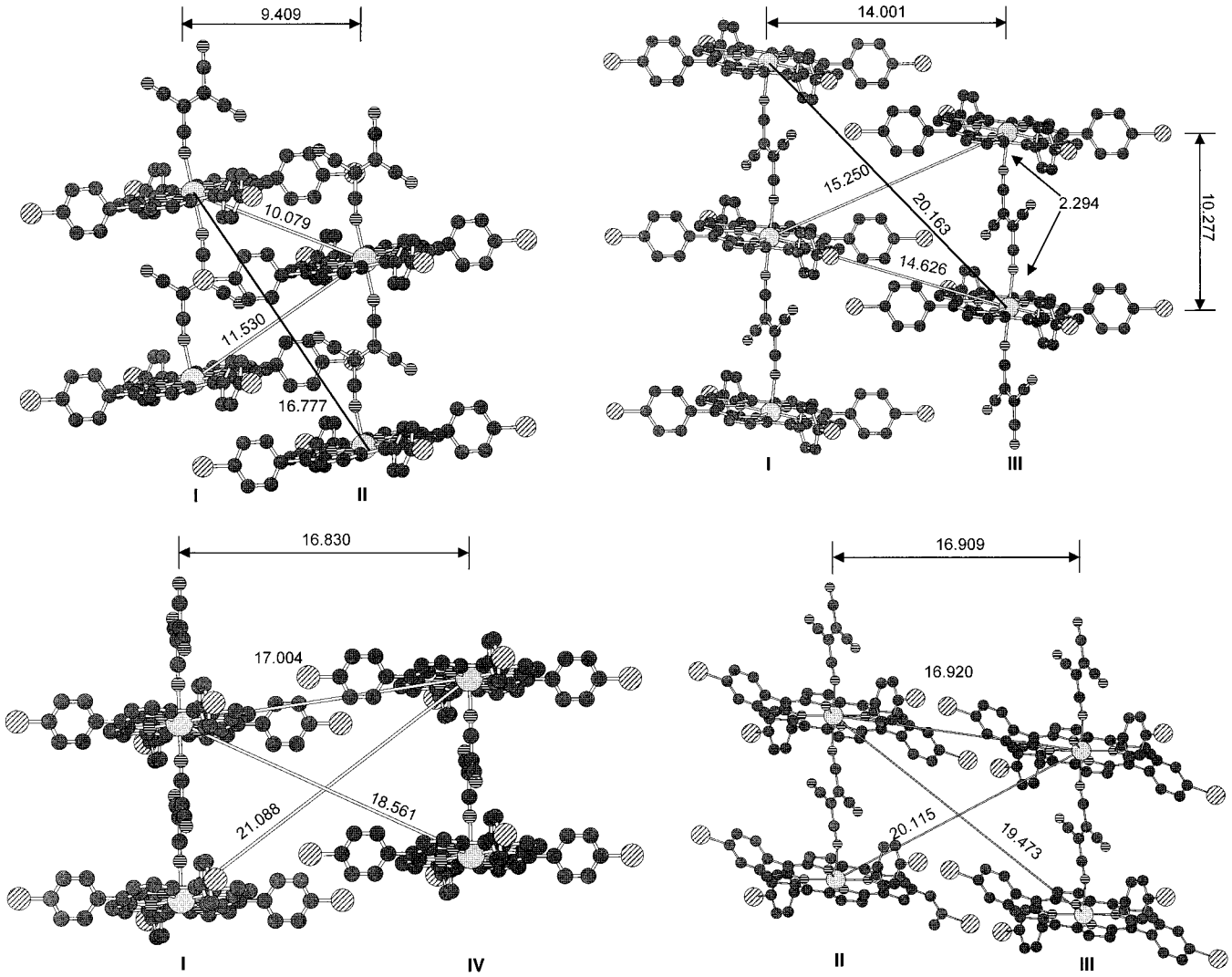

Figure 3. View of key inter- and intrachain interactions between unique chains **I**, **II**, **III**, and **IV** for [MnTBrPP][TCNE]·2PhMe (**1Br**). Note the $[TCNE]^{\bullet-}$ *trans*-μ-*N*-σ-bonding to $[MnTBrPP]^{+}$ and the uniform chains. The hydrogen atoms and the toluene solvates have been omitted for clarity.

1F, **1Cl**,[7e] **1Br**, and **1I**, respectively (Figure 6) ($T > 150$ K for **1F** and **1Br** and 150 K $< T <$ 190 K for **1I**). Unfortunately a satisfactory Seiden fit was not obtained for **1Br**; instead the shape and position of the χT minimum was used as a guide to estimate J_{intra}. These values compare well with reported values for [MnTPP][TCNE], [MnTOMePP][TCNE], and [MnToFPP]-[TCNE] of -115, -32, and -64 K, respectively.[7e,f] These fits predict 102,[7e] 85, and 158 K T_{min} values, which are in good agreement with the observed values of 110,[7e] 80, and 160 K for **1Cl**,[7e] **1Br**, and **1I**, respectively. The predicted T_{min} of 670 K for **1F** cannot be experimentally tested. Hence, these J_{intra}'s and T_{min}'s are consistent with antiferromagnetic coupling decreasing as **1F** > **1I** > **1Cl** ~ **1Br**. The anomaly with **1I** is again attributed to the aforementioned differing structure.

The intrachain coupling, J_{intra}, may also be approximated by the relationship $J_{intra} = -T_{min}/4.2$ for $H = -2J_{intra}\mathbf{S}_a\cdot\mathbf{S}_b$.[27] J_{intra}/k_B for **1Cl**,[7e] **1Br**, and **1I** is -26, -19, and -38 K, respectively. Using the T_{min} estimated from the Seiden expression for **1F**, 670 K, J_{intra} was estimated to be -160 K. The predicted values for this model are lower than those of the Seiden expression by $\sim 2^{1/2}/2$ as noted earlier;[7e] however, the magnitude of the coupling follows the same tendency for both predictions.

The ferrimagnetic nature of this system may also be realized from the magnetization values at 2 K and 50 000 Oe, Figure 7, Table 5. The data for **1F**, **1Cl**,[7e] **1Br**, and **1I** are consistent with an antiferromagnetically coupled $S_{Tot} = 2 - {}^1/_2 = {}^3/_2$ system (i.e., an expected saturation magnetization, M_s, of 16 755 emu Oe/mol) and are substantially lower than the expectation for ferromagnetic coupling, i.e., a M_s of 27 925 emu Oe/mol for an $S_{Tot} = 2 + {}^1/_2 = {}^5/_2$ system. The reduced saturation observed in the present case may be attributed to spin canting in the system due to single-ion anisotropy of Mn^{III}.

The onset of higher dimensional ordering (i.e., 2- and 3-D) was examined by the in-phase, $\chi'(T)$, and out-of-phase, $\chi''(T)$, components of the zero-field-cooled ac susceptibility, $\chi_{ac}(T)$, Figure 8. The ordering temperature, T_c, is determined from the maxima in the $\chi'(T)$ data taken at 10 Hz, and is 28.0, 8.8, 8.0, and 6.5 K for **1F**, **1Cl**, **1Br**, and **1I**, respectively.[28] Concomitantly, maxima in $\chi''(T)$ (10 Hz) were observed at 28.0 and 5.8

(27) Drillon, M.; Coronado, E.; Georges, R.; Gianduazzo, J. C.; Curely, J. *Phys. Rev. B* **1989**, *40*, 10992. This relationship has been obtained from a numerical model that considers the exact quantum nature of the $S = 2$ spin; hence discrepancies with the classical Seiden model reflect the limitations imposed when the $S = 2$ spin is taken as a classical spin.

(28) An ordering temperature, T_c, can also be determined by the divergence or bifurcation of the zero-field-cooled, field-cooled magnetization at low field. These T_c's, determined at 1 Oe, are 28.5, 8.1, and 5.3 K for **1F**, **1Br**, and **1I**, respectively, in good agreement with the T_c's obtained from $\chi'(T)$ at 10 Hz.

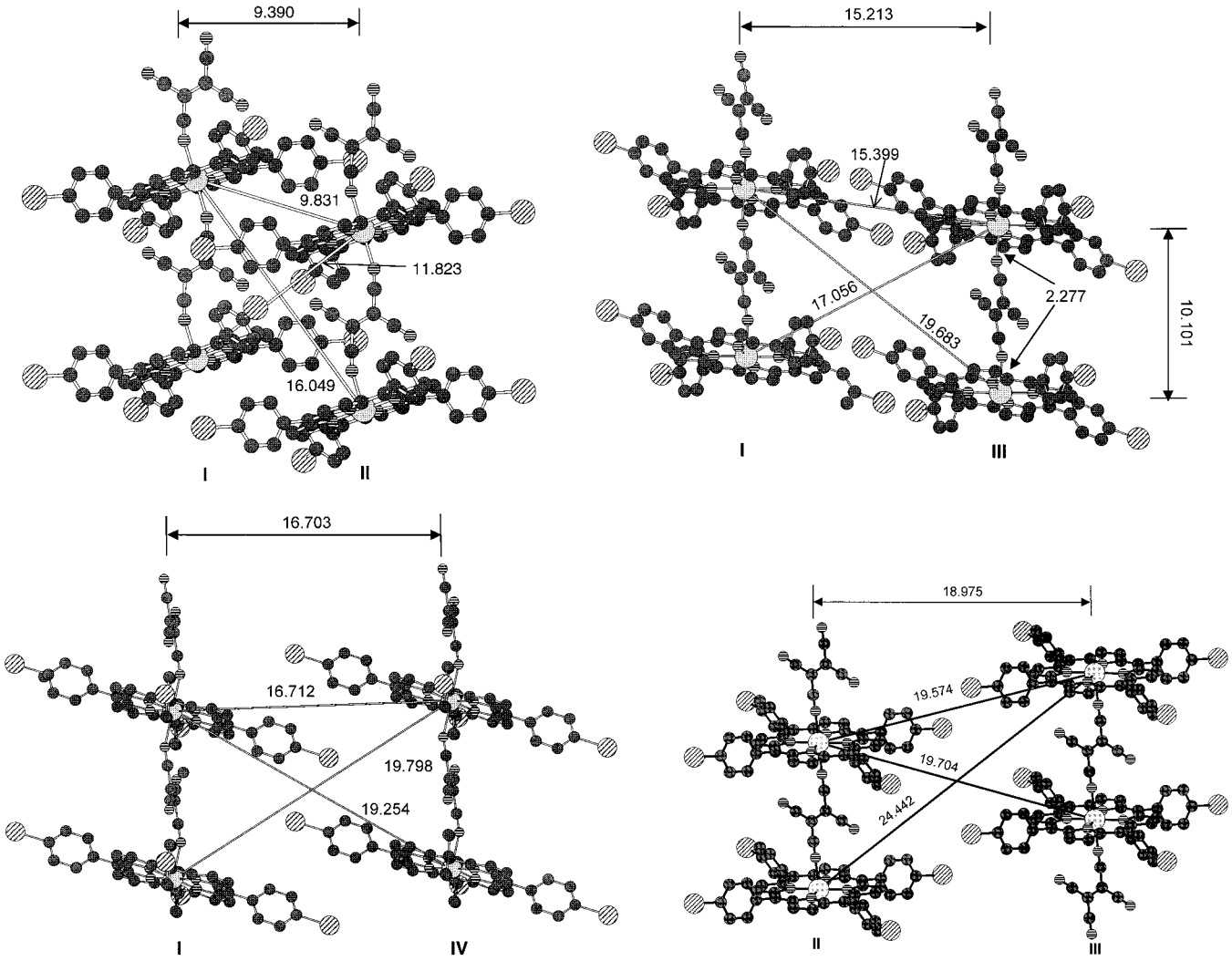

Figure 4. View of key inter- and intrachain interactions between unique chains **I**, **II**, **III**, and **IV** for [MnTIPP][TCNE]·2PhMe (**1I**). Note the $[TCNE]^{\bullet-}$ *trans-μ-N-σ*-bonding to $[MnTIPP]^{+}$ and the uniform chains. The hydrogen atoms and the toluene solvates have been omitted for clarity.

Table 4. Key Mn···Mn Distances (Å) for [MnTXPP][TCNE]·2PhMe [X = Cl (**1Cl**), Br (**1Br**), I (**1I**)]

	layer (see text)	Mn···Mn (axis)	Mn···Mn		
1Cl[a]	intra **I**, **II**, **II′**	10.171 (*a*)	11.458	17.077	
	inter **I**, **III**, **IV**	14.522 (*c*)	16.610	18.360	19.554
1Br	intra **I**, **II**, **II′**	10.079 (*a*)	11.530	16.777	
	inter **I**, **III**, **IV**	14.626 (*c*)	15.250	16.920	17.004
1I	intra **I**, **II**, **II′**	9.831 (*a*)	11.823	16.049	
	inter **I**, **III**, **IV**	15.399 (*c*)	16.712	17.056	19.254

[a] Reference 7e.

K for **1F** and **1I**, respectively. In contrast, **1Cl** and **1Br** exhibit two distinct maxima in χ'' at 5.8 and 7.1 K (**1Cl**) and 5.8 and 7.1 K (**1Br**); however, in each case the peaks in $\chi''(T)$ are consistent with the presence of an uncompensated moment.

For **1F**, symmetrical frequency independent peaks in both $\chi'(T)$ and $\chi''(T)$ components of χ_{ac} centered at 28.0 K were observed. To date this is the highest reported T_c of any porphyrin-based magnet, significantly higher than those previously reported for [MnTPP][TCNE]·2PhMe at 14 K[5] or $[MnTOC_{12}H_{25}PP][TCNE]$·2PhMe at 21.4 K.[9a] Unlike **1F**, the $\chi_{ac}(T)$ behavior of **1Br** was characterized by two transitions in $\chi'(T)$, the first a frequency independent peak centered at 8.0 K lacking a corresponding $\chi''(T)$ component and the second a frequency dependent peak near 6.0 K with a corresponding peak in $\chi''(T)$. Similar behavior was observed for **1Cl** with the first and second peaks in χ'(T) centered at 8.8 and ~7.1 K, respectively.[7e] The nature of two similar transitions has been extensively studied in $[MnOEP][C_4(CN)_6]$; however, a clear understanding in the present system has not yet been realized.

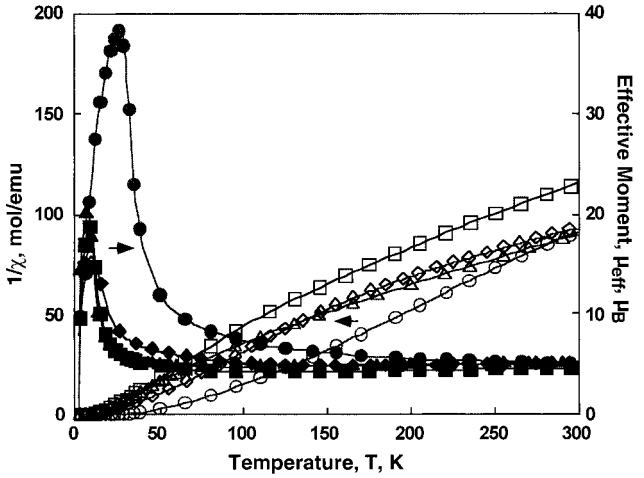

Figure 5. Reciprocal molar magnetic susceptibility, χ^{-1} (open symbols), and moment, μ_{eff} (closed symbols), as a function of temperature (1000 Oe) for [MnTFPP][TCNE]·*x*PhMe (○, ●), [MnTClPP]-[TCNE]·2PhMe (□, ■), [MnTBrPP][TCNE]·2PhMe (△, ▲), and [MnTIPP][TCNE]·2PhMe (◇, ◆).

Table 5. Summary of Magnetic Data for [MnTXPP][TCNE]·2PhMe [X = H (**1H**), F (**1F**), Cl (**1Cl**), Br, (**1Br**), I (**1I**)]

	μ_{eff}, μ_B	θ, K	θ' K	M_s (5 T, 2 K), emu Oe/mol	T_{min}, K	J_{intra}, K[b,c]		$\lvert J_{inter}\rvert$ mK		T_c,[d] K	ϕ	T_c,[e] K	H_c (2 K), kOe	H_{cr} (2 K) kOe
								a, *c*	*b*, *c*					
1F	5.12	*f*	70	17 000	670[a]	−225	−160	32.1	45.4	28.0	0.005	28.5	21.8	20.0
1Cl[7e]	4.55	−60	13	11 000	110	−33	−26	29.9	26.4	8.8	0.017		6.8[h]	6.7[i]
1Br	5.44	−53	13	12 500	80	−30	−19	18.9	29.9	8.0	0.005	8.1	4.1	4.0
1I	5.08	−79	30	11 000	160	−53	−38	7.2	9.8	6.5	0.17	5.3	15.8	15.9
1H	5.12	*f*	61	16 000[j]	270	−115	−64	3.7	27.2	14.0	0.18		30[k]	

[a] From the Seiden expression. [b] From T_{min}/4.2 (see text). [c] From eq 2. [d] Taken from the maximum in $\chi'(T)$ at 10 Hz. [e] Taken as the bifurcation temperature at 1 Oe (see text). [f] Not observed. [g] Reference 7e. [h] Reference 35. [i] Reference 31. [j] Reference 5. [k] Reference 36.

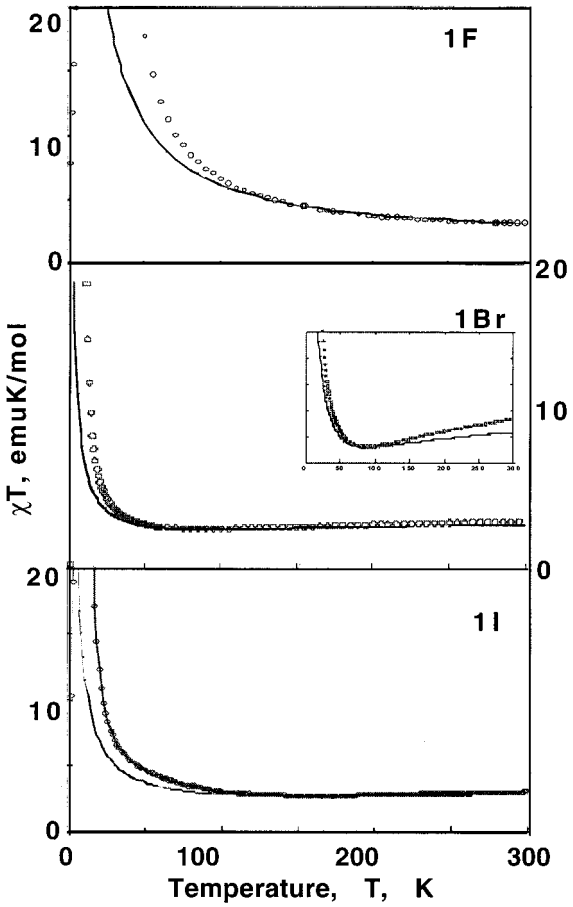

Figure 6. Fit of the $\chi T(T)$ data (solid lines) to the Seiden expression[14] for [MnTFPP][TCNE]·*x*PhMe (**1F**), [MnTBrPP][TCNE]·2PhMe (**1Br**), and [MnTIPP][TCNE]·2PhMe (**1I**).

On the basis of the details of the [MnOEP][$C_4(CN)_6$] studies, we believe that the first transition is antiferromagnetic in nature, possibly arising from interlayer interactions and the second frequency dependent peak in $\chi'(T)$ due to the onset of weak 3-D ferromagnetism.[29] The frequency dependence of the low-temperature $\chi'(T)$ peak is indicative of disorder or frustration in the spin lattice suggestive of a spin glass or superparamagnetic state.[5b,30,31]

Although structurally similar to **1Cl** and **1Br**, the $\chi_{ac}(T)$ behavior of **1I** is unique in the series. **1I** exhibits a single broad frequency dependent maximum at 6.5 and 5.7 K, $\chi'(T)$ and $\chi''(T)$, respectively, that is similar to that of [MnTP′P][TCNE]·2PhMe[7a] and [MnTOMePP][TCNE]·2PhMe.[7f] The origin of the spin−lattice frustration in **1Cl**, **1Br**, and **1I** maybe attributed to disorder in the orientation of the toluene solvate or other structural disorder below the ∼15% detection limit of diffraction experiments. The observed disorder may be parametrized by $\phi = \Delta T_c/[T_c\Delta(\log \omega)]$,[31] where ϕ ranges from 0.0047 (**1F**) to 0.17 (**1I**), indicating that **1I** exhibits the highest degree of disorder.

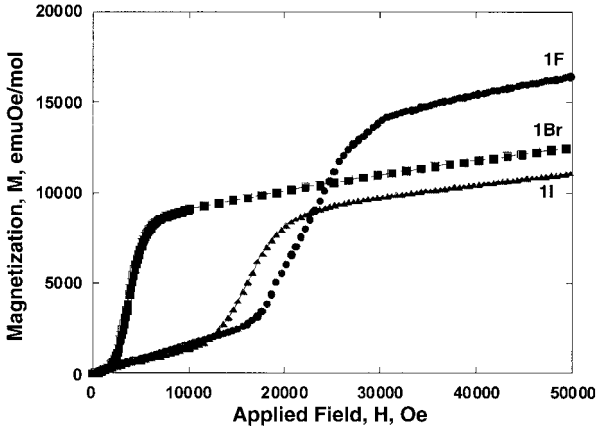

Figure 7. Field dependencies of the magnetization, $M(H)$, at 2 K for [MnTFPP][TCNE]·*x*PhMe (●), [MnTBrPP][TCNE]·2PhMe (■), and [MnTIPP][TCNE]·2PhMe (▲).

The 2 K $M(H)$ data are characteristic of metamagnetic behavior, i.e., a slow rise in $M(H)$ with increasing H until a critical field, H_c, is reached and then a rapid rise of the moment to a values of M_s near saturation for **1F**, **1Cl**,[7e] **1Br**, and **1I**. Observed values of H_c range from 4.1 (**1Cl**) to 21.8 kOe (**1F**) (Table 5) in accord with that for **1Cl** and [MnTPP][TCNE]·2PhMe, 30 kOe.[28] No evidence of metamagnetic behavior is evident above 5 K for **1Cl**, **1Br**, and **1I**; therefore, the metamagnetic transition temperature, T_c, for **1Cl**,[7e] **1Br**, and **1I** is between 4 and 5 K with **1F** exhibiting metamagnetic behavior below 10 K. These T_c's cannot be more precisely identified from either $d\chi(T)/dT$ or $d\chi T(T)/dT$ plots as maxima ascribable to these transitions are not discernible. This perhaps is a consequence of transitions to other magnetically ordered phases above this T_c, which are not present for simpler systems such as $[Me_3NH]Co^{II}Cl_3\cdot H_2O$ (T_c = 4.13 K; H_c = 650 Oe at 3.75 K)[32] and $[Fe^{III}(C_5Me_5)_2][TCNQ]$ (TCNQ = 7,7,8,8-tetracyano-*p*-quinodimethane) (T_c = 2.55 K; H_c = 1.6 kOe).[33]

At 2 K hysteresis, again characteristic of metamagnetic behavior, with coercive fields, H_{cr}, is observed for **1F**, **1Cl**,[7e] **1Br**, and **1I**, Figure 9. The coercive fields range from 4.0 kOe for **1Br** to 20.0 kOe for **1F**, Table 5. This extremely high coercive field that is observed for **1F** is the largest value reported

(29) (a) Wynn, C. M.; Gîrtu, M. A.; Miller, J. S.; Epstein, A. J. *Phys. Rev. B.* **1997**, *56*, 14050. (b) Wynn, C. M.; Gîrtu, M. A.; Sugiura, K.-I.; Brandon, E. J.; Manson, J. L.; Miller, J. S.; Epstein, A. J. *Synth. Met.* **1997**, *85*, 1695. (c) Wynn, C. M.; Gîrtu, M. A.; Miller, J. S.; Epstein, A. J. *Phys. Rev. B* **1997**, *56*, 315. (d) Epstein, A. J.; Wynn, C. M.; Brinckerhoff, W. B.; Miller, J. S. *Mol. Cryst. Liq. Cryst.* **1997**, *305*, 321.

(30) (a) Gîrtu, M. A.; Wynn, C. M.; Sugiura, K.-I.; Miller, J. S.; Epstein, A. J. *J. Appl. Phys.* **1997**, *81*, 4410. (b) Gîrtu, M. A.; Wynn, C. M.; Sugiura, K.-I.; Miller, J. S.; Epstein, A. J. *Synth. Met.* **1997**, *85*, 1703.

(31) Mydosh, J. A. *Spin Glasses*; Francois and Taylor: Washington, DC, 1993.

(32) Spence, R. D.; Botterman, A. C. *Phys. Rev.* **1974**, *B9*, 2993.

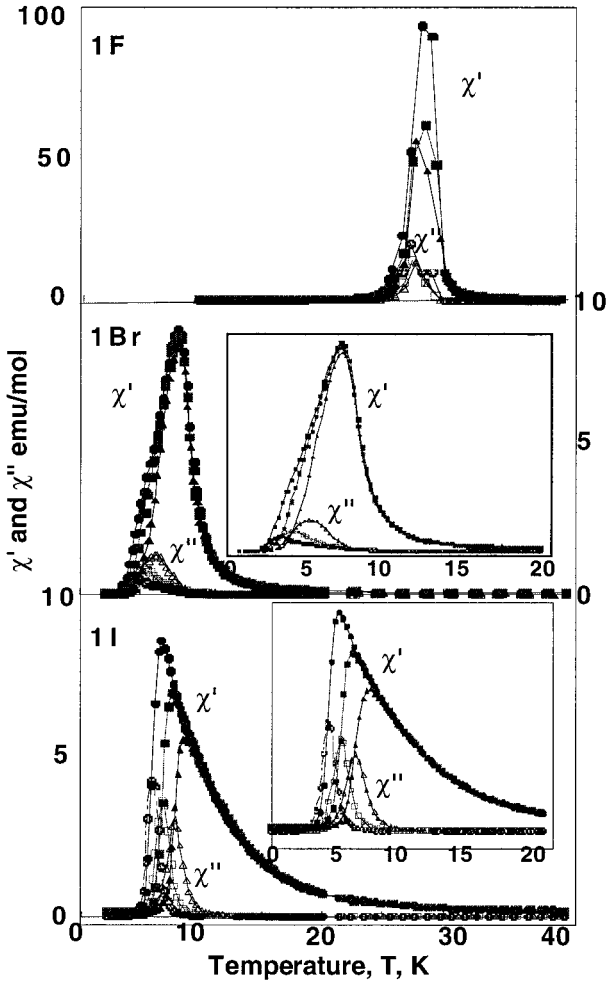

Figure 8. Dispersive, χ' (●, ■, ▲) and absorptive, χ''(○, □, △), components of the ac susceptibility at 10, 10^2, and 10^3 Hz, respectively, for [MnTFPP][TCNE]·*x*PhMe (**1F**), [MnTBrPP][TCNE]·2PhMe (**1Br**), and [MnTIPP][TCNE]·2PhMe (**1I**).

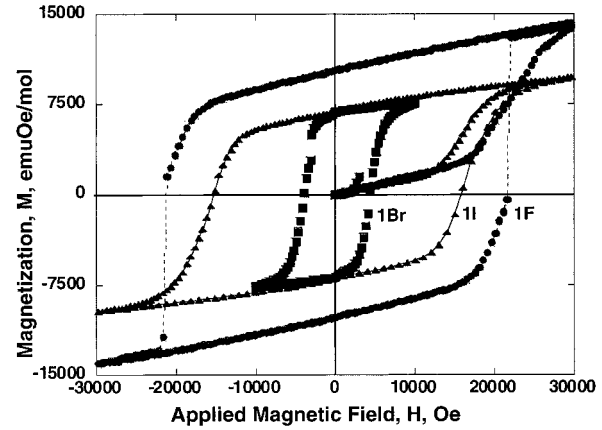

Figure 9. Hysteretic behavior at 2 K for [MnTFPP][TCNE]·*x*PhMe (○), [MnTBrPP][TCNE]·2PhMe (■), and [MnTIPP][TCNE]·2PhMe (▲).

for this class of material.[6−10] Further studies are under investigation to understand the high coercive field as well as this unprecedented transition.

Exchange Coupling. The T_c, as obtained from the maxima in χ'(T, 10 Hz), for the [MnTXPP][TCNE]·2PhMe family decreases as **1F** (28 K) > **1Cl** (8.8 K) ≈ **1Br** (8.0 K) > **1I** (6.5 K), as T_c is proportional to J.[34,35,36] The dominant antiferromagnetic intrachain (1-D) coupling, J_{intra}, is reflected in T_{min},

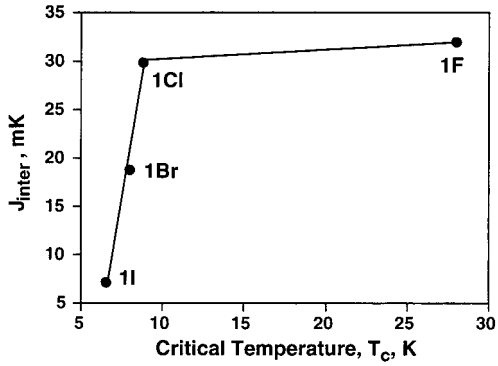

Figure 10. Correlation between T_c and J_{inter} calculated from eq 2 using J_{intra} calculated from the Seiden expression (see text).

the temperature at which a minimum $\chi T(T)$ occurs, which increases with J_{intra}, or can be modeled by the complex Seiden expression[14] or the simpler Curie−Weiss constant θ, or $J_{intra} = -T_{min}/4.2$ expression, Table 5.[27] Independent of which of these four models is used, J_{intra} decreases as **1F** > **1I** > **1Cl** ∼ **1Br** and does not correlate with the aforementioned trend in T_c, Table 5.

Since T_c and values for J_{intra} are determinable, J_{inter} can be calculated from eq 2. Two J_{inter} values were calculated using the Seiden model[14] and the relationship $J_{intra} = -T_{min}/4.2$,[27] Table 5. The observed trend for T_c, i.e., **1F** > **1Cl** > **1Br** > **1I**, is only obtained for J_{inter} when calculated from eq 2 using J_{intra} calculated from the Seiden model, Table 5. This correlation, although monotonic, is not linear for the series [MnTXPP]-[TCNE] (X = F, Cl, Br, I), Figure 10. The substantial deviation from nonlinearity for the **1F** point may be due to some yet to be determined structural feature. The unusual nature of **1F** is also noted by the unexceptionally large θ value, but the highest T_c observed for this family of magnets.

To establish a structure−function relationship requires detailed structural information, which is lacking for **1F**, but is available for the similarly structured **1Cl**, **1Br**, and **1I**. The new data for **1Br** and **1I** is consistent with the previous correlation between T_{min} and θ' as a function of the dihedral angle between the MnN_4 and $[TCNE]^{\bullet-}$ mean planes,[13] Figure 11. This is a 1-D magneto−structural correlation as it relates only the intrachain interactions with structural features and leads to the identification of the σ overlap between the Mn d_{z^2} and the $[TCNE]^{\bullet-}$ p_z orbital providing the magnetic coupling.

The establishment of a 3-D magneto−structural correlation that could be used to predict T_c has been elusive. Attempts to correlate T_c with *a*- and *c*-axis lengths, (i.e., the interchain Mn···Mn separations, lead to a correlation with *c*, but not with *a*.

Conclusion

The ditoluene solvates of [MnTXPP][TCNE] (X = Cl, Br, I) have been prepared and formed structurally similar, but not

(33) Candela, G. A.; Swartzendruber, L. J.; Miller, J. S.; Rice, M. J. *J. Am. Chem. Soc.* **1979**, *101*, 2755.
(34) Van Vleck, J. H. *The Theory of Electric and Magnetic Susceptibilities*; Oxford University Press: London, 1932. Van Vleck, J. H. *Rev. Mod. Phys.* **1945**, *17*, 7. Van Vleck, J. H. *Rev. Mod. Phys.* **1953**, *25*, 220. Goodenough, J. B. *Magnetism and the Chemical Bond*; John Wiley & Sons (Interscience): New York, 1963.
(35) Reassessment of the $\chi''(T)$ data for **1Cl** reveals a double peak with maxima at both 5.8[7e] and 7.1 K as well as a metamagnetic critical field, H_c, of 6800 Oe and a coercive field, H_{cr}, of 6700 Oe.
(36) Zhou, P.; Morin, B. G.; Epstein, A, J.; McLean, R. S.; Miller, J. S. *J. Appl. Phys.* **1993**, *73*, 6569. Brinckerhoff, W. B.; Morin, B. G.; Brandon, E. J.; Miller, J. S.; Epstein, A. J. *J. Appl. Phys.* **1996**, 79, 6147.

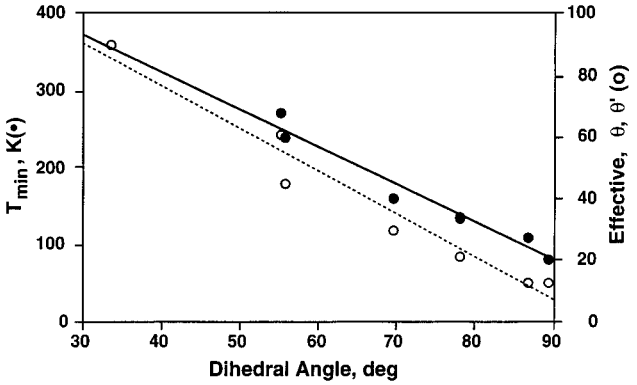

Figure 11. Correlation of the dihedral angle, ϕ, between the MnN_4 and $[TCNE]^{\bullet-}$ mean planes with the temperature at which χT has a minimum, T_{min}, and the effective θ value, θ'.

isomorphous, 1-D coordination polymers. [MnTFPP][TCNE] (**1F**) exhibits an ordering temperature of 28.0 K and has been structurally elusive. This T_c is ~33% higher than the next highest T_c for a member of this family and twice as great as that for the typical member of this family of magnets. Furthermore, in comparison to other members of this family of magnets, it has minimal spin glass behavior. Hence, detailed magnetic measurements as well as further attempts to obtain single crystals suitable for X-ray studies are in progress. Additionally, the 70 K θ for **1F** is substantially lower than the 93 and 90 K values reported for $[Mn^{III}TF_4OMePP][TCNE]\cdot 2PhMe$ (H_2TF_4OMePP = tetrakis[2,3,5,6-tetrafluoro-4-methoxyphenyl]porphyrin)[5g] and $[Mn^{III}TP'P][TCNE]\cdot 2PhMe$,[5a] respectively, although the latter have substantially lower T_c's of 10.3 and 15 K, respectively. Hence, a correlation between θ and T_c due to the complex nature of the structure and magnetic transitions does not presently exist.

Acknowledgment. The authors appreciate the constructive comments and insight provided by E. J. Brandon, A. J. Epstein, C. M. Wynn, and M. Gîrtu (The Ohio State University). We also thank M. T. Johnson for preparing H_2TIPP and A. M. Arif for crystallographic studies, and we gratefully acknowledge the support in part from National Science Foundation Grants CHE9320478 and CHE9730948, and Grant CHE9807669 enabling the acquisition of the CCD diffractometer.

Supporting Information Available: A summary of the crystallographic data, tables of fractional coordinates and isotropic thermal parameters, anisotropic thermal parameters, bond distances and angles, and intramolecular nonbonding distances for [MnTBrPP][TCNE]·2PhMe and [MnTIPP][TCNE]·2PhMe. This material is available free of charge via the Internet at http://pubs.acs.org.

IC990170G